ELSEVIER

Journal of Power Sources 81–82 (1999) 637–641

JOURNAL OF POWER SOURCES

www.elsevier.com/locate/jpowsour

Performance and characterization of lithium–manganese-oxide cathode material with large tunnel structure for lithium batteries

Y. Yang *, D. Shu, J.K. You, Z.G. Lin

State Key Lab for Physical Chemistry of the Solid Surface and Department of Chemistry, Xiamen University, Xiamen, 361005, China

Abstract

The synthesis, structure characterization and electrochemical performance of novel todorokite electrode materials (tunnel size: 3×3) for lithium batteries have been studied in this paper. It is shown by means of XRD that synthesized materials (e.g., Mg^{2+}-containing sample) have todorokite structure. It is also found that the reversibility of the Li^+ insertion process into the todorokite materials decreased after acid treatment due to removal of Mg^{2+} from the tunnel and the breakdown of the tunnel structure during the following intercalation/deintercalation cycles. The electrochemical impedance spectra (EIS) for todorokite electrode materials are measured and simulated. It was measured that the apparent diffusion coefficient (D_{Li+}) of todorokite material is at a level between 10^{-7} and 10^{-10} cm^2/s by use of potential-step electrochemical spectroscopy.

Keywords: Lithium ion batteries; Lithium–manganese oxides; Large-tunnel structure

1. Introduction

In the development of cheaper and environmental benign cathode materials for a new class of Li-ion batteries, manganese oxides are attractive and competitive. Extensive studies [1,2] have been done on numerous manganese oxide compounds in the last decades for this purpose. However, the performance of manganese oxides are not satisfactory compared with that of commercial lithium–cobalt oxides either with regard to cycle stability or practical capacity, thus deep insight and systematic understanding of the relationships between structure and performance (especially the cyclic stability) of manganese oxides material are desirable, assuming that the era of wide commercialisation of the material could come.

It is well known that many manganese oxides have different characteristic tunnels in their structures. However, the properties and structural changes of the characteristic tunnels for manganese oxides during the intercalation/deintercalation processes have not been fully understood [3]. For example, what are the effects of the size of tunnel and the metal ions existing in the tunnel on the performance of the oxides, how about the changes and stability of tunnels during the intercalation process, etc. Thus the detailed study of the electrochemical properties and cyclic stability of the manganese oxides with novel layer- and tunnel-structure will be significant [3,4]. In this work, the investigation of the electrochemical behaviour of manganese oxides with large tunnel structure (i.e., todorokite structure, tunnel size: 3×3) and containing different cations (i.e., Mg^{2+}, Ni^{2+} and Co^{2+}) in the tunnels have been done. Some interesting results about this novel electrode material will be reported in this paper.

2. Experimental

The synthesis of manganese oxides with large tunnel structure is based on literature methods [5] with some modifications, i.e., the Na^+-birnessite was first prepared using the reaction between 0.5 M $Mn(NO_3)_2$ and NaOH under the flow of oxygen bubbles into the solution. Then the Na^+-birnessite was exchanged with different chloride salt solutions (i.e., 1 M $MgCl_2$, $CoCl_2$ etc.) for more than 24 h. The final step for synthesis of todorokite material was based on the hydrothermal reaction of Mg^{2+}-birnessite or Ni^{2+}-birnessite, etc. in an autoclave reactor at about 160°C. The advantage of hydrothermal synthesis of intercalation electrode materials is apparent [6]: firstly, it can be synthesized at low temperature (between 100° and 200°C); it is quite convenient to change synthesis conditions such

* Corresponding author. Tel.: +86-592-218-39-05; Fax: +86-592-208-53-49; E-mail: yyang@xmu.edu.cn

0378-7753/99/$ - see front matter
PII: S0378-7753(99)00235-9

as pH, temperature and the cations in the solution, the latter may act as the structure-directing species, or template, to change the composition of compounds. In addition, the synthesized samples through hydrothermal processes are crystalline materials, which can be used as electrode materials directly, avoiding heat treatment of the material at high temperature during the preparation process. The elemental analysis of the samples indicated that molecular formula for Mg^{2+}-containing compounds is $Mg_{0.847}Na_{0.092}Mn_{6.31}O_{12} \cdot 5.33H_2O$. The main electrochemical instruments used in this paper are a PARC 273 potentiostat (USA) or IM6 impedance analyser (Germany). The cell-assembling or treatment of Li metal were carried out in Mbraun Model-100 inert-gas chamber. The counter and reference electrodes were pure Li foil electrodes. The electrolyte solution was 1 M $LiClO_4$ + PC + DME (Newcast Chemical Reagent, Beijing, China). Other experimental details have been described in a previous paper [7]. The determination of apparent diffusion coefficients of Li^+ in the todorokite materials is based on the method first proposed by Thompson [8,9], i.e., electrochemical voltage spectroscopy (EVS) or potential-step electrochemical spectroscopy. The amplitude of potential step is 10 mV/h, and current–decay curves are recorded simultaneously after the potential step.

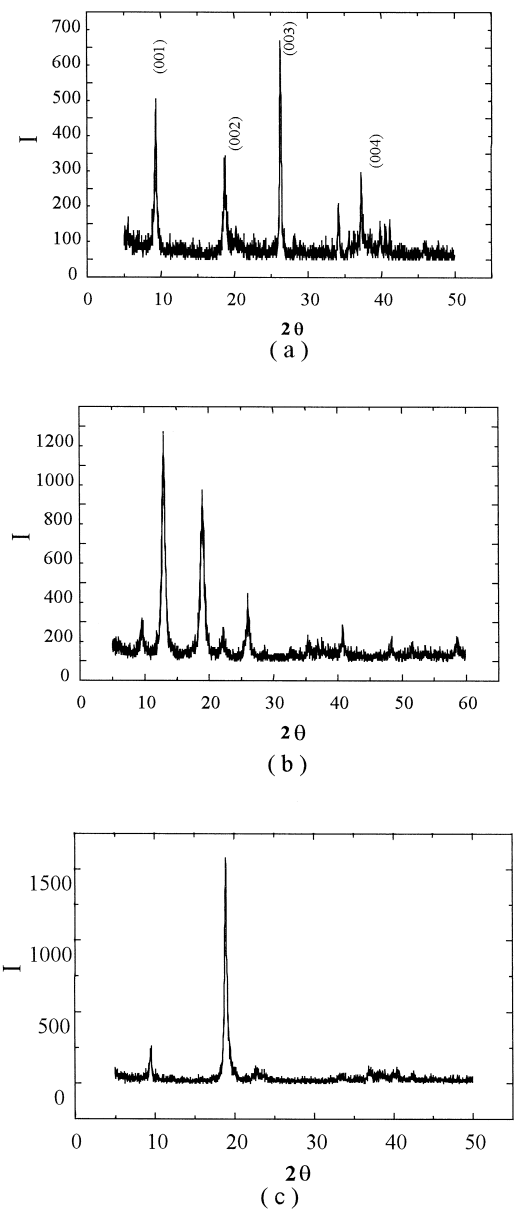

Fig. 1. X-ray diffraction (XRD, Cu as target sources, scan rate: 8°/min) graphs of synthesized products containing different cations through hydrothermal processes. (a) Mg^{2+}, (b) Ni^{2+}, (c) Co^{2+}.

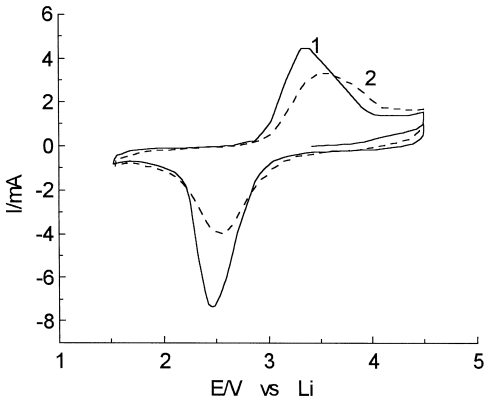

Fig. 2. Cyclic voltammograms of Mg^{2+}-todorokite electrode materials in 1 M $LiClO_4$ + PC + DME; scan rate is 0.2 mV/s. The number shown in each curve represents cycle numbers.

3. Results and discussions

3.1. Structural characterization of todorokite materials with and without acid pretreatment

Fig. 1(a–c) shows the XRD graphs of synthesized products containing different M^{2+}-birnessites ($M = Mg^{2+}$, Co^{2+} and Ni^{2+}) in the hydrothermal processes. It is shown that similar todorokite structure of the materials can be obtained with addition of Mg^{2+} in the ion-exchange

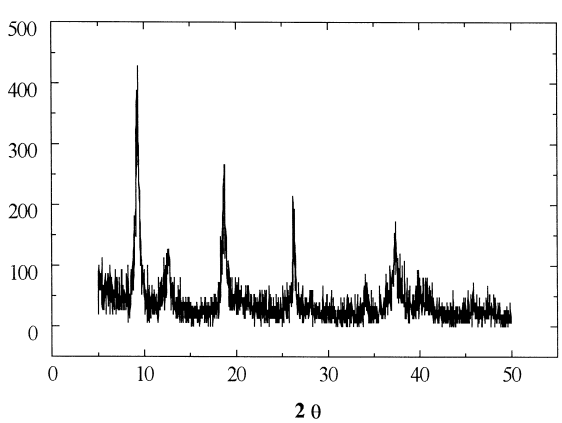

Fig. 3. XRD graph of Mg^{2+}-todorokite electrode materials after acid treatment.

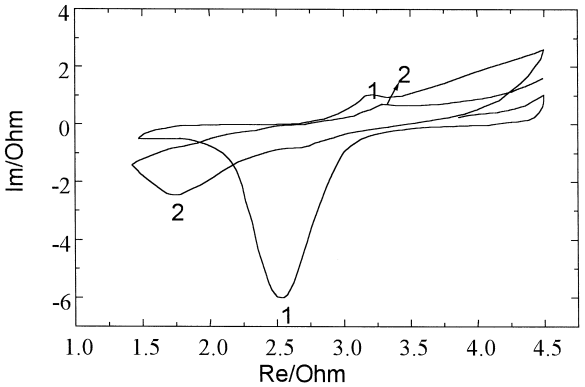

Fig. 4. Cyclic voltammograms of acid-treated Mg^{2+}-todorokite electrode materials in 1 M $LiClO_4$ + PC + DME; scan rate is 0.2 mV/s. The number shown in each curve represents cycle numbers.

process (Fig. 1a), quite similar to that reported in the literature [10]. Here, the four peaks at 0.95, 0.47, 0.34 and 0.24 nm are indexed as (001), (002), (003) and (004) diffraction, respectively by assuming that todorokite materials has a pseudo-orthorhombic cell [5]. However, it should be noted that if we hope to prepare a high-quality todorokite product we must get high-quality Na^+-birnessite for hydrothermal synthesis at first. It is found that the quality of Na^+-birnessite in our method is greatly dependent on synthesis temperature, i.e., it is demonstrated that low temperature ($\sim 0°C$) is suitable for the synthesis of high-quality Na^+-birnessite. In addition, when the Mg^{2+} ions were replaced by Ni^{2+} and Co^{2+} in the first ion-exchange processes, the synthesized products still have characteristic peak (i.e., $2\theta = 9.5°$, corresponding to (001) crystal face) for todorokite structure. It is also shown that there is some distortion in the todorokite structure of the materials while with addition of Co^{2+} and Ni^{2+} (Fig. 1b,c). Fig. 2 shows cyclic voltammograms of Mg^{2+}-todorokite at scan rate of 2 mV/s. It can be observed that a couple of current peaks at 3.4 V and 2.6 V which correspond to the deintercalation/intercalation of Li ions of the todorokite materials. In the previous paper [6], it was reported that todorokite material has quite high discharge capacity at about 125 mA h/g after four cycles. Some samples which have todorokite structure have shown good performance in cycle-stability (it will be reported elsewhere). More important in this work, we have also investigated the structural changes of Mg^{2+}-todorokite after treatment with dilute nitric acid solution. Fig. 3 shows the XRD graph of Mg^{2+}-todorokite after acid treatment. Fig. 4 shows cyclic voltammograms of treated samples in 1 M $LiClO_4$ + PC + DME. From the voltammograms, a large reduction peak can be observed for Li^+-intercalation potential in the first potential cycle and then it decreased greatly in the following cycles. However, the oxidation peak for deintercalation of Li^+-ions is small even in the first cycles, indicating the difficulty of deintercalation of Li^+-ions after intercalation. However, both oxidation and reduction peaks for deintercalation and intercalation processes of Li^+ became much smaller from the second potential cycle for acid-treated samples. Based on the above results, it is proposed that the main structure is still kept after the acid treatment; however, the performance of the treated sample is not good and thus it is suggested that Mg^{2+} in tunnel is dissolved from the tunnel and results in the deterioration of the electrochemical performance of the materials.

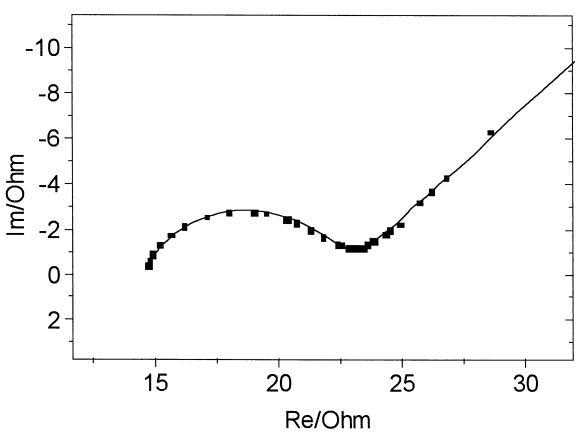

Fig. 5. A typical electrochemical impedance spectrum of Mg^{2+}-todorokite electrode materials when $x = 1$ at open circuit potential. The dotted spots represent experimental results, the solid line represents simulation results (for simulation details, see Table 1).

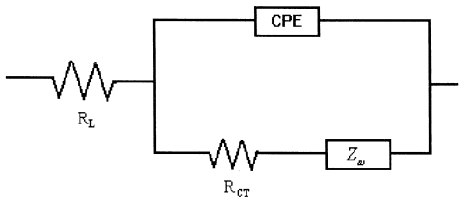

Fig. 6. An equivalent circuit diagram for simulation of electrochemical impedance spectra of the todorokite electrode materials.

3.2. Electrochemical characterization of todorokite electrode materials by means of electrochemical impedance spectra (EIS) and EVS

In this work, the electrochemical properties of the novel todorokite electrode materials have been characterised by

Table 1
Simulation results for electrochemical impedance spectra of todorokite electrode materials at different intercalation ratios x

x	E (V)	R_L	R_{CT} (Ω)	W (Ω/s$^{1/2}$)	CPE (μF)	α	D_F	E_r (%)
0	3.36	14.2	5.32	16.4	15.3	0.852	2.17	0.1
1	2.845	14.5	8.12	16.2	11.2	0.765	2.31	0.1
2	2.734	14.5	11.17	31.6	9.4	0.669	2.49	0.2
3	2.61	14.9	11.37	53.8	7.7	0.685	2.46	0.2
2	2.94	14.6	9.02	60.7	11.5	0.677	2.48	0.2
1	3.284	14.4	9.11	14.9	18.9	0.631	2.58	0.2
0	3.586	13.9	7.79	12.8	21.9	0.631	2.58	0.2

E is stable open-circuit potential. E_r is error deviation in the simulation. The significance of other parameters listed are explained in the text.

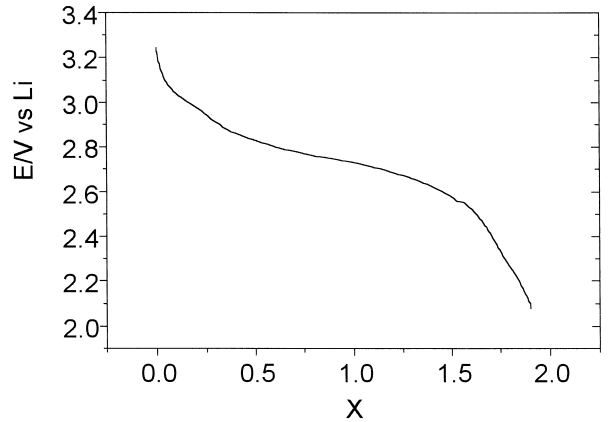

Fig. 7. The relationship between equilibrium open-circuit potential and intercalation ratio x for todorokite electrode materials.

means of different electrochemical and spectroscopic methods (e.g., X-ray photoelectron spectroscopy). For example, we have investigated the electrode kinetics of the new electrode materials by using EIS and EVS. Fig. 5 shows a typical electrochemical impedance spectrum (Nyquist plot) when the electrode material was discharged to $x = 1$ ($Li_xMMn_yO_z$, M is represented by Mg^{2+}, etc.). It is found that there were few differences in characteristic EIS except in amplitude between different x values (when $0 \leq x \leq 3$). Apparently, the Nyquist plot (Fig. 5) can be simulated using normal equivalent circuit containing elements such as R_L (solution resistance), R_{CT} (charge-transfer or reaction resistance), Z_W (Warburg impedance) and CPE (constant-phase element). $Z_{CPE} = K(j\omega)^{-\alpha}$ (K is the constant, α is correlated with fractual dimension parameter, and $\alpha = 1/(D_F - 1)$. Here, D_F is fractual dimensions. The adapted equivalent circuit diagram is shown in Fig. 6. The simulated values for the circuit elements at different values of x are also tabulated in Table 1. From the table, it is shown that R_{CT} increased with the x, it suggests that intercalation of lithium ions into the material could cause the decrease of the electronic conductivity of the material

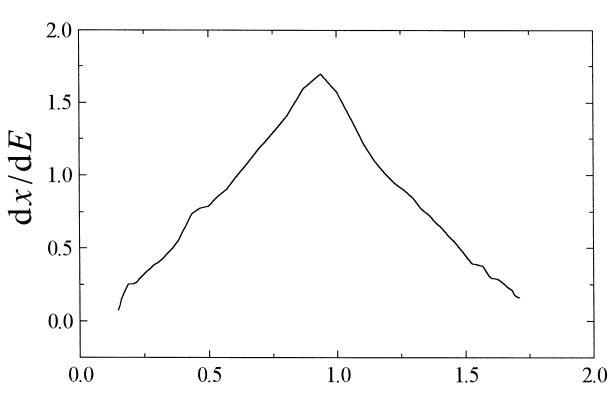

Fig. 8. The relationship between dx/dE and x for todorokite electrode materials.

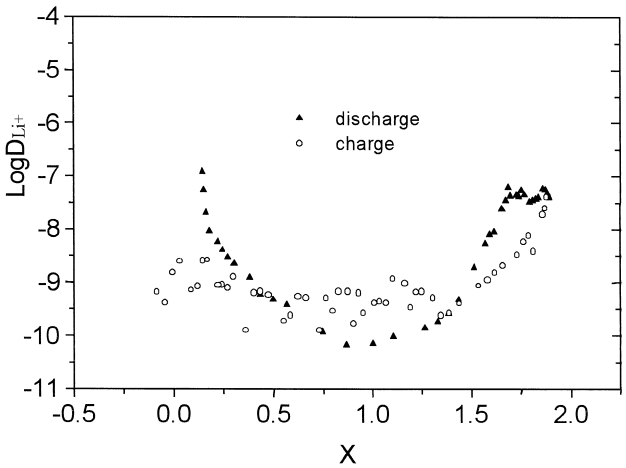

Fig. 9. The relationship between log D_{Li+} (D_{Li+} is apparent diffusion coefficients of the materials) and x for charging (circle) and discharging (triangle) processes, respectively.

due to the enlargement of lattice in the crystal materials after the Li^+ intercalation. In addition, the Z_{CPE} (also D_F in the simulation) decreased with the proceeding of the intercalation process. This suggests that roughness of the material increased after intercalation/deintercalation cycles. Since apparent diffusion coefficient (D_{Li+}) of the electrode material is an important kinetic parameter for intercalation process. We have also used electrochemical potential spectroscopy to investigate the quasi-equilibrium intercalation process of lithium ions in todorokite material and measure the corresponding parameters for the first time. Figs. 7–9 shows that $E \sim x$, $dx/dE \sim x$ and log $D_{Li+} \sim x$ for Mg^{2+}-todorokite electrode materials, respectively. From Fig. 7, it is shown that there are no two plateaus in $E \sim x$ curve (when x is changed from 0 to 2), implying a quite homogeneous Li^+-intercalation process. The shape of the $dx/dE \sim x$ curve (Fig. 8) looks like the shape of an up–down 'V', also similar to that normal intercalation system [11]. From Fig. 9, it is observed that apparent diffusion coefficients (D_{Li+}) of the electrode materials is dependent of the depth of discharge state (i.e., intercalation concentration of Li^+ in the electrodes, or x). The apparent diffusion coefficient (D_{Li+}) of todorokite material is at a level between 10^{-7} and 10^{-10} cm^2/s. The distribution of D_{Li+} with x is quite stable whether for charging or discharging processes except when x approaches the limit (i.e., $x = 0$).

4. Conclusions

The synthesis, structural characterization and electrochemical performance of novel todorokite materials (tunnel size: 3×3) have been studied. It is found that the reversibility of insertion process of Li^+ into the todorokite materials containing Mg^{2+} in the tunnels decreased after

diluted nitric acid treatment which may be due to removal of Mg^{2+} from the tunnel and the breakdown of the tunnel structure during intercalation/deintercalation cycles. The electrochemical impedance spectra for todorokite electrode materials are measured and simulated. The measured apparent diffusion coefficient (D_{Li+}) of todorokite material is at a level between 10^{-7} and 10^{-10} cm^2/s using EVS.

Acknowledgements

Financial support from Natural Science Foundation of Fujian Province, Ministry of Education and New-Material Division, National High-Technology Research and Development Committee of China are greatly appreciated.

References

[1] M.M. Thackeray, Prog. Solid State Chem. 25 (1997) 1–71.
[2] P.G. Bruce, Chem. Commun. (1997) 1817.
[3] G. Pistoria et al., J. Electrochem. Soc. 144 (1997) 1502.
[4] Z.R. Tian, Y.G. Yin, S.L. Suib, C.L.O. Young, Chem. Mater. 9 (1997) 1126.
[5] Y.F. Shen, R.P. Zerger et al., Science 260 (1993) 511.
[6] M.S. Whittingham, Curr. Opin. Solid State Mater. Sci. 1 (1996) 227.
[7] Y. Yang, D. Shu, H. Yu, X. Xia, Z.G. Lin, J. Power Sources 65 (1997) 227.
[8] A.H. Thompson, Phys. Rev. Lett. 23 (1978) 1551.
[9] A.H. Thompson, J. Electrochem. Soc. 126 (1979) 608.
[10] Y.F. Shen, S.L. Suib, C.L.O. Young, J. Am. Chem. Soc. 116 (1994) 11020.
[11] W.R. McKinnon, in: P.G. Bruce (Ed.), Solid State Electrochemistry, Chap. 7, Cambridge Univ. Press, 1995.